chinaXiv:202112.00015v1

Using statistical models and GIS to delimit the groundwater recharge potential areas and to estimate the infiltration rate: A case study of Nadhour-Sisseb-El Alem Basin, Tunisia

Ali SOUEI[1,2*], Taher ZOUAGHI[3]

[1] Georesources Laboratory, Water Researches and Technologies Center (WRTC) of Borj Cedria, Soliman 8020, Tunisia;
[2] Department of Geology, FST, University of Tunis El Manar, Tunis C P 2092, Tunisia;
[3] Department of Geo-Exploration Techniques, Faculty of Earth Sciences, King Abdulaziz University, Jeddah 21589, Saudi Arabia

Abstract: The water resources of the Nadhour-Sisseb-El Alem Basin in Tunisia exhibit semi-arid and arid climatic conditions. This induces an excessive pumping of groundwater, which creates drops in water level ranging about 1–2 m/a. Indeed, these unfavorable conditions require interventions to rationalize integrated management in decision making. The aim of this study is to determine a water recharge index (WRI), delineate the potential groundwater recharge area and estimate the potential groundwater recharge rate based on the integration of statistical models resulted from remote sensing imagery, GIS digital data (e.g., lithology, soil, runoff), measured artificial recharge data, fuzzy set theory and multi-criteria decision making (MCDM) using the analytical hierarchy process (AHP). Eight factors affecting potential groundwater recharge were determined, namely lithology, soil, slope, topography, land cover/use, runoff, drainage and lineaments. The WRI is between 1.2 and 3.1, which is classified into five classes as poor, weak, moderate, good and very good sites of potential groundwater recharge area. The very good and good classes occupied respectively 27% and 44% of the study area. The potential groundwater recharge rate was 43% of total precipitation. According to the results of the study, river beds are favorable sites for groundwater recharge.

Keywords: potential recharge; remote sensing; statistical models; MCDM; Nadhour-Sisseb-El Alem Basin

1 Introduction

Groundwater is a development element in the dry area around the Mediterranean that naturally appeared as a particularly sensitive domain of the constraints of supply in fresh water. Moreover, increasing water demand due to agricultural, urban and industrial development, greatly stressed the water resources. In the future, water overexploitation will aggravate water shortages and cause social, economic and food security problems, especially in the southern Mediterranean countries. The groundwater resources are highly sensitive to human activities and climatic conditions (Jaiswal et al., 2003; Yeh et al., 2009, 2016).

Tunisian state has succeeded, since the 1990s, to mobilize 90% of the potential water resources

(Ayadi, 2014). Despite this success in the integrated administration of hydraulic resources, the hydrological situation of the country has been always ready to the risk of water scarcity in the years to come (Ayadi, 2014).

The delineation of groundwater recharge areas and the estimation of the natural recharge rate are important areas of research to avoid water shortages in the future. The results obtained using GIS in scientific research have attracted the attention of researchers in the fields of water resources. The use of Geographic Information System (GIS) tools in the research of the groundwater recharge area has heightened from early 1990s (Krishnamurthy et al., 2000; Jha et al., 2007; Kallali et al., 2007; Tweed et al., 2007; Chenini et al., 2010; Riad et al., 2011a, b; Yeh et al., 2016). GIS-based mapping can provide precise data concerning the spatial distribution. Remote sensing coupled with statistical models, such as Multi-criteria decision-making (MCDM) and analytic hierarchy process (AHP), are largely used in water resources investigation (Jha et al., 2007; Madrucci et al., 2008; Preeja et al., 2011; Rahman et al., 2012; Rashid et al., 2012; Jasrotia et al., 2013; Yeh et al., 2016).

Intensive exploitation of groundwater resources resulting from social and economic development in the Nadhour-Sisseb-El Alem Basin has caused a piezometric drop of 20 m, during the last decade in some areas of the basin (Souei et al., 2018). This indicates that Nadhour-Sisseb-El Alem Basin is highly sensitive to groundwater level fluctuation. These critical situations involve interventions to rationalize the integrated management of water resource in the basin. The use of efficient tools such as GIS and remote sensing coupled with statistical methods is required for sustainable development of water resources in the basin. Therefore, statistical study is required to establish a relationship between factors having impacts on the groundwater recharge to take into account the impact of each factor in the water recharge index.

The objectives of this study are the delimitation of the groundwater recharge area from the WRI and the determination of the potential groundwater recharge rate in the Nadhour-Sisseb-El Alem Basin. The factors that affect groundwater recharge are evaluated. The weights of the factors are determined and analyzed using the MCDM, AHP and Fuzzy logic. The maps of the spatial distribution of factors are completed based on the GIS and remote sensing tools and methods.

2　Materials and methods

2.1　Study area

The study was performed in the Nadhour-Sisseb-El Alem Basin (39°45′50″–40°20′00″N, 11°01′40″–11°25′30″E; Fig. 1), Tunisia. It is characterized by a Mediterranean climate with an irregular rainfall and long dry periods with a mean annual precipitation of 150–330 mm (GWRD, 2013a) and potential mean annual evapotranspiration of 1500 mm. The annual mean temperature is about 20°C.

The area of Nadhour-Sisseb-El Alem Basin is 1946 km^2 and consists of 27 sub-basins (Souei and Zouaghi, 2017). Streams are sporadic due to the lack of runoff for most of the year. Special hydrological characteristics, insufficient sporadic flows and floods produce rare torrential and turbid flows that lead to generally endorheic systems. The Nadhour-Sisseb-El Alem Basin has four hill dams (Ogla, Sehel, Kseb and Saidaine, and great Nebhana Dam) and more than 40 hilly lakes.

The Nadhour-Sisseb-El Alem Basin includes multilayered aquifer system composed of deep and phreatic aquifers (Souei, 2019). The phreatic aquifers correspond to sandy-conglomerate deposits of Quaternary age (Fig. 2). The deep aquifers are stored in the Oligocene and Miocene-Quaternary series. Aquifer system is very prone to seasonal piezometric level fluctuations which are closely linked to rainfall natural recharge. The groundwater usually flows from the northwest to southeast. The pumping tests show that transmissivity varies between $2.2×10^{-3}$ and $8.5×10^{-3}$ m^2/s. The permeability, calculated by the product of the aquifer thickness and transmissivity, varies between $0.34×10^{-4}$ and $3.34×10^{-4}$ m/s. From the hydrogeological aspect, the basin is divided into three connected sub-basins according to its main structural framework (Souei et al., 2018; Souei and Zouaghi, 2018) (Fig. 2). The first sub-basin is in the Nadhour region marked by thickness Oligocene and Neogene-Quaternary deposits. The second one is in the Sisseb region presenting a high domain

characterized by thinning of Miocene-Quaternary and low Oligocene series (Souei et al., 2021). The third one is in El Alem region corresponding to a subsiding zone with a thick Mio-Plio-Quaternary series, which is about 2 km. Artificial recharge is $25×10^6$ m^3 in the period 1992–2013 (GWRD, 2013b).
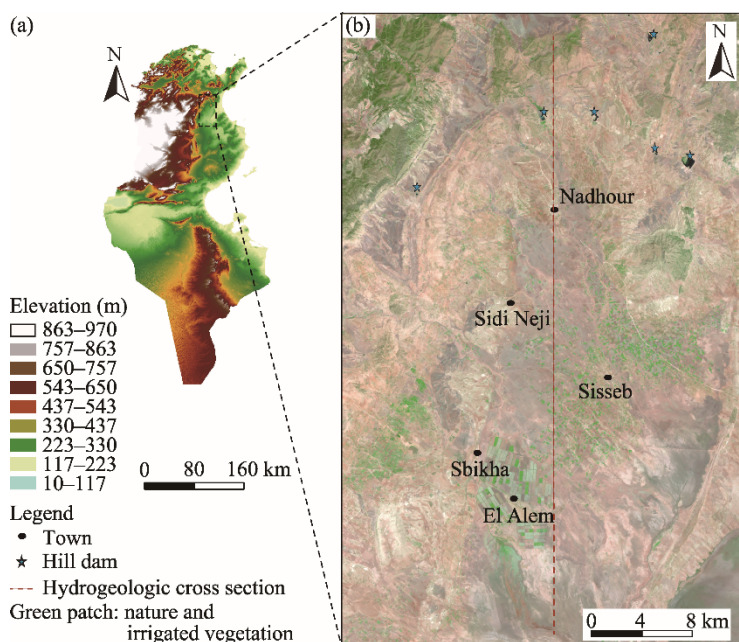

Fig. 1 Location (a) and Landsat image (resolution 30 m) (b) of the study area, Nadhour-Sisseb-El Alem Basin, Tunisia
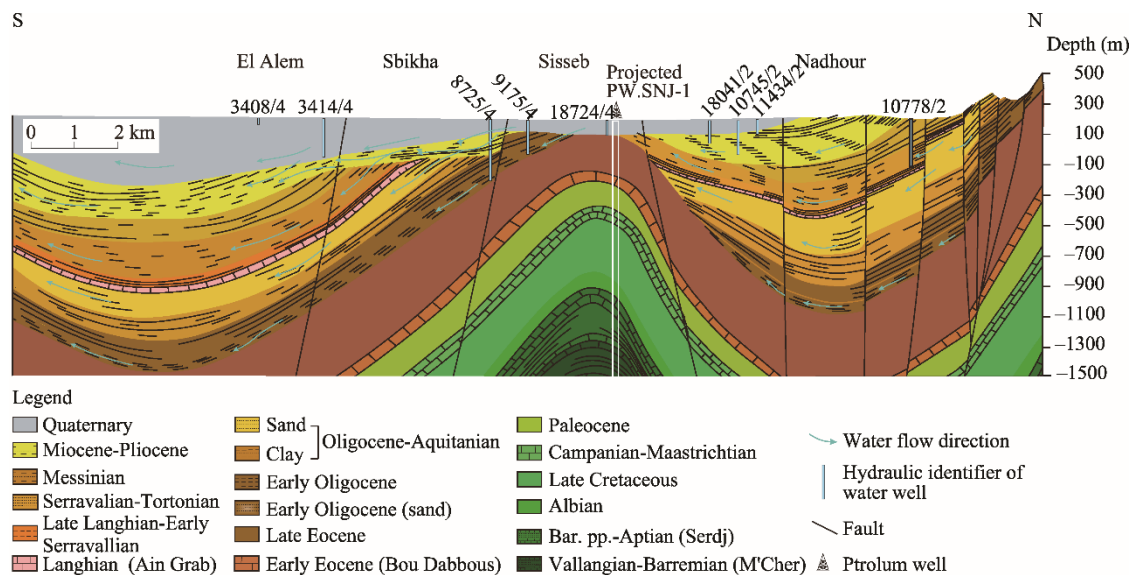

Fig. 2 Hydrogeologic cross section of the aquifer system in Nadhour-Sisseb-El Alem Basin modified from Souei et al. (2018). S, south; N, north.

Water resources are exploited to supply the drinking water, industrial and agricultural sectors. The exploitation of groundwater grows from $16×10^6$ m^3 in 1976 to $23×10^6$ m^3 in 2013. The intense pumping has lowered the groundwater level, which is around 40 m in some areas. (Souei, 2012; Souei et al., 2018; Souei and Zouaghi, 2018). This has influenced the water supply.

2.2 Methods

Data used in this study includes the Landsat 8 satellite images (23 October 2017), shuttle radar topography mission (SRTM), pedological map with a scale of 1:500,000, the Jebel Fkirine, Enfidhaville, Jbebina, SidiBou Ali, AinJloula and SebkhaKelbia geological maps with a scale of 1:50,000. Remote sensing technique can be used to improve location accuracy and make precise mapping (Aouragh et al., 2016). In this work, we identified eight factors, lithology, soil, slopes, topography, land cover and use, drainage, lineaments and runoff, which affect the potential groundwater recharge. The use of GIS has achieved several thematic maps that characterize the study area. The method used in this study (Fig. 3) corresponds to a succession of steps for the automatic extraction of hydrographic network, lineaments and slope. The digitalization technique of geological maps was chosen to identify lithology. The data provided by the various GIS tools are used after a correction of the result, with reference to field data, topographic and geological maps.
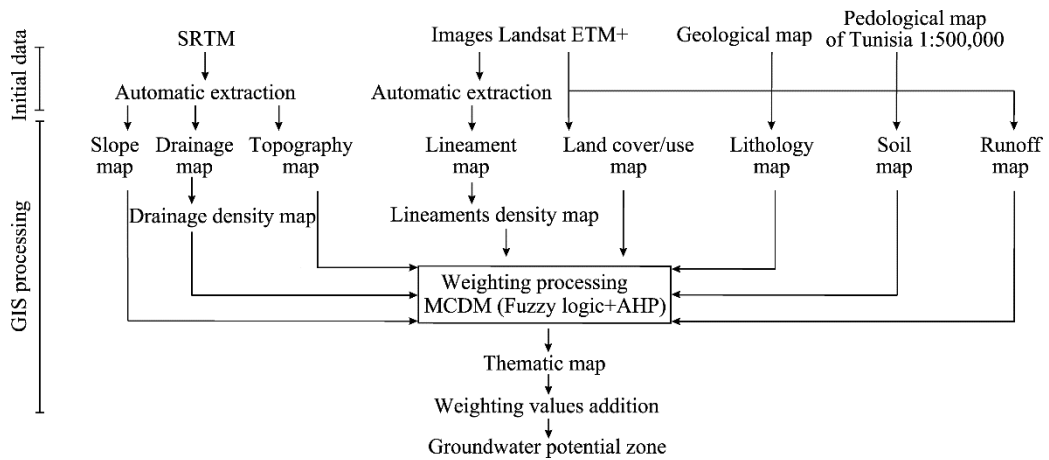

Fig. 3 Processing chain of making potential zone map for groundwater by using GIS and remote sensing SRTM (shuttle radar topography mission)

For more precision in the results and its spatial distribution, the study area was subdivided in grids of 500 m×500 m. Within each grid, the necessary data have been added. The recharge map was obtained by the sum of the weights of the eight parameters.

$$\mathrm{WRI} = \sum_{i=1}^{n} \mathrm{ER}_i , \qquad (1)$$

$$\mathrm{ER} = \mathrm{PR} \times \mathrm{RW} \times \mathrm{AR} \times W , \qquad (2)$$

where WRI is the water recharge index; ER_i is the effective rate for each map; i is a factor; n is the number of factors; PR is the proposed rate; RW is the proposed relative weight; AR is the assigned rate; and W is AHP weight.

Firstly, the factors that influence the groundwater recharge related to the study area were determined in reference to the published scientific and technical guideline documents. In the first stage the order of importance of every factor was established. Figure 4 shows the relationship among the factors and illustrates their influence and interaction. The order of importance of every factor was determined based on the influence of each factor in the relationship. The weight 1 was assigned to a major effect and the weight 0.5 was assigned to a minor effect (Shaban et al., 2006). RW of every factor (i) is the addition of the number of major effect (x) and number of minor effect (y) of this factor (RW$_i$=x_i×major effect+y_i×minor effect), the results are showed in Table 1.

Then, the each factor was subdivided into classes describing the domain of effect. Each class was expressed by a numerical value, expressing their order of importance by using fuzzy logic (Zadeh, 1965) instead of Saaty scale (Saaty, 1980). Fuzzy logic presents an extension of classical set theory (Leberling, 1981; Buckley, 1984). The classical logic represents the membership of an

element by true (if the element belongs) or false (if the element does not belong) (Zadeh, 1965). Fuzzy logic replaces the degree membership, of proposition, represented in true/false by a degree of membership (Zadeh, 1987) in the interval [0, 1] (Rezaei et al., 2013). The non-membership is represented by 0, the total membership is represented by 1, and the partial membership is represented by values between 0 and 1 (Saaty, 1980). Fuzzy logic also allows us to move from a linguistic ranking (very good, moderate, very low, ...) to a numerical ranking. If A is a class of the set μ in fuzzy logic, the membership relation is determined as $\mu A = U \rightarrow [0, 1]$, and the order of intervention is between 0 and 1.

The weight of factors is obtained by the establishment of the interactive interrelationship diagram of various factors (Shaban et al., 2006). The interrelationship diagram is suitably revised based on expert consulting, international published guidelines and scientific documents. The AHP method is used to determinate the contribution and occurrence of each factor (Saaty, 1980). The rate for each class is assigned according to the Fuzzy set theory (Zadeh, 1965).
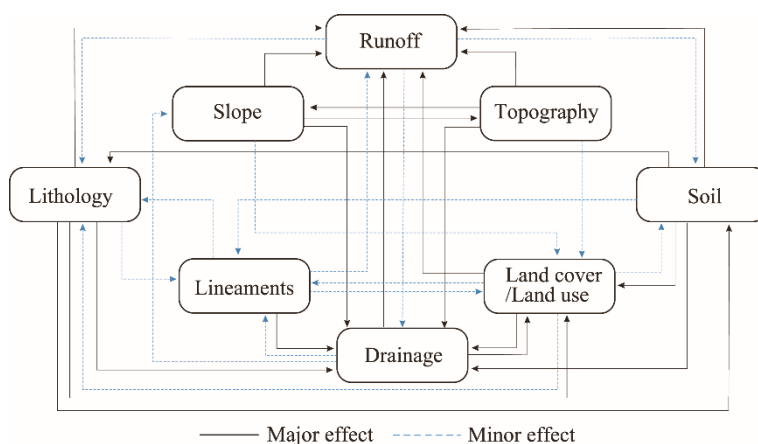

Fig. 4 Major and minor relationship among factors influencing the potential groundwater recharge

Table 1 Proposed relative weight (RW) obtained from the relationships among factors influencing the potential groundwater recharge

Factor	Calculation process	RW
Lithology (Li)	4×1+1×0.5	4.5
Soil (S)	4×1+1×0.5	4.5
Slope (Sl)	3×1+1×0.5	3.5
Topography (T)	3×1+1×0.5	3.5
Land cover/land use (LU/C)	2×1+3×0.5	3.5
Drainage density (Dd)	2×1+2×0.5	3.0
Lineaments density (Ld)	1×1+3×0.5	2.5
Runoff (Ru)	0×1+3×0.5	1.5

Note: Calculation process is $RW_i = x_i \times$major effect$+y_i \times$minor effect, where i is the factor; x is the number of major effect and y is the number of minor effect of this factor.

In this study, fuzzy logic in linear function was applied in the determination of the PR of each class. AR was determined by RW multiply PR.

In the third step, the W of a factor was chosen according to the linear method using AHP method (Saaty, 1980). A matrix of pair-wise comparisons was determined and it was a reciprocal matrix. Referring to the order of importance of factors deduced previously from the membership relation, the matrix calculation was made by dividing the importance value of a factor in the row by the importance value of a factor in the column. W was determined (Eqs. 3 and 4) by the normalization of the sum of each row by the total of the matrices; the results are showed in Table 2. ER of each class was determined by W multiply PR.

Table 2 Comparison matrix obtained for eight factors for the analytic hierarchy process (AHP)

Factor	Li	S	Sl	T	LU/C	Dd	Ld	Ru	W
Li	1.0								0.17
S	4.5	1.0							0.17
Sl	3.5	3.5	1.0						0.13
T	3.5	3.5	3.5	1.0					0.13
LU/C	3.5	3.5	3.5	3.5	1.0				0.13
Dd	3.0	3.0	3.0	3.0	3.0	1.0			0.11
Ld	2.5	2.5	2.5	2.5	2.5	2.5	1.0		0.10
Ru	1.5	1.5	1.5	1.5	1.5	1.5	1.5	1.0	0.06

Note: W is the AHP weight.

$$W_k = \frac{L_k}{\sum_{i=1}^{n} L_i}, \tag{3}$$

$$L_k = \sum_{i=1}^{n} \frac{RW_k}{RW_i} + 1, \tag{4}$$

where n is the number of factors; i is a factor; L_k is the sum of the line of factor k; L_i is the total of the sum of lines; and RW is the proposed relative weight.

The matrix reliability was determined by calculation of the consistency ratio (CR) which was deduced from the consistency index (CI) (Saaty, 1980).

Indeed if CR>0.1, the decision set could be too inconsistent to be powerful (Saaty, 1980). In practice, CR>0.1 occasionally has to be admitted. If CR=0.0, it means that the decision is absolutely reliable (Saaty, 1980).

The CI is a measure of the departure from consistency and it is calculated as follows:

$$CI = \frac{\gamma - n}{n - 1}, \tag{5}$$

$$\gamma = \left(\sum_{j=n}^{n} \left(L_j / W_j \right) \right) / n, \tag{6}$$

where γ is the average value of the consistency vector; L is the consistency vectors of factor j; W is the AHP weight of factor j; and n is the eight influencing factors.

Finally, a sensitivity analysis parameter was determined. This technique was applied to evaluate the efficiency of the potential groundwater recharge index map carried out using the eight parameters (Eq. 9). Sensitivity analysis of the single parameter (Napolitano and Fabbri, 1996) was an achievement to control the impact of the factors in the potential groundwater recharge index. This inspection was accomplished by comparing "effective" and assigned "AHP weight" weight of each factor (Singh et al., 2015).

$$W_{pi} = \left(P_{ri} \times P_{wi} / V \right) \times 100, \tag{7}$$

where W_{pi} is the effective weight (%); P_{ri} is the rating of respective parameters; P_{wi} is the weight of parameters; and V is the final vulnerability index.

3 Results

3.1 Factors influencing groundwater recharge

3.1.1 Lithology

Lithology is a significant factor influencing groundwater recharge by guiding the water penetration (Elewa and Qaddah, 2011). The lithology map was extracted from a geological map with a scale of 1:50,000. The lithology map makes it possible to determine the favorable infiltration zone. The relief areas, formed by a calcareous crust, show a weak infiltration. Salty depressions, formed by clays, silts and evaporites, are unfavorable to infiltration. The lithology can also control the

drainage density and fracturing intensity by affecting the time of concentration of the waters in the basin (Kirpich, 1940) and control the secondary porosity.

The PR of the lithology was determined. The alluviums and gravel sand admitted a PR value of 1.00 and marls had a PR value of 0.00. PR values of the other classes were between 0.00 and 1.00 (Table 3).

Table 3 Classes and ratings for determining potential groundwater recharge zones

Factor	Classes	PR	RW	AR	W	Effective rate (ER)
Li	Marls and sandy marls	0.15		0.68		0.11
	Limestone and dolomites	0.43	4.5	1.94	0.17	0.33
	Sand and sandstone	0.63		2.84		0.48
	Alluviums and gravelly sand	1.00		4.50		0.76
S	Building	0.07		0.32		0.05
	Hydromorphic and allomorphic soils	0.15		0.68		0.11
	Poor soil	0.52	4.5	2.34	0.17	0.40
	Rendzine soil	0.83		3.74		0.63
	Mineral soil and wadi beds	1.00		4.50		0.76
Sl	0.0−3.4	1.00		3.50		0.46
	3.4−9.4	0.78	3.5	2.73	0.13	0.36
	9.4−18.0	0.58		2.03		0.27
	18.0−44.0	0.04		0.14		0.02
T	400−500	0.20		0.70		0.09
	300−400	0.40		1.40		0.18
	200−300	0.60	3.5	2.10	0,13	0.28
	100−200	0.80		2.80		0.37
	0−100	1.00		3.50		0.46
LU/C	Building	0.06		0.21		0.03
	Forest	0.24		0.84		0.11
	Agricultural and waste land	0.65	3.5	2.28	0.13	0.30
	Surface water body	1.00		3.50		0.46
Dd	0.00−0.62	1.00		3.00		0.34
	0.62−1.25	0.50	3.0	1.50	0.11	0.17
	1.25−1.87	0.20		0.60		0.07
	1.87−2.50	0.02		0.06		0.01
Ld	0−10	0.22		0.60		0.06
	10−30	0.66	2.5	1.65	0.10	0.16
	30−45	1.00		2.50		0.24
Ru	Building	0.07		0.11		0.01
	Marls and clay	0.19		0.29		0.02
	Limestone and dolomites with fractures	0.52	1.5	0.78	0.06	0.04
	Sand and sandstone	0.65		0.98		0.06
	Alluviums	0.81		1.22		0.07
	Wadi beds	1.00		1.50		0.08

Note: PR, proposed rate; RW, proposed relative weight; AR, assigned rate; W, AHP weight.

The lithology map shows that the areas formed by sand, sandstone and wadi beds were the most favorable to the infiltration (Fig. 5). The central parts of the basin, formed by sand, sandstone and wadi beds were moderately favorable. The areas of relief, formed by a limestone crust, had low infiltration. Salted depressions formed by clays, silts and evaporites were unfavorable to infiltration.
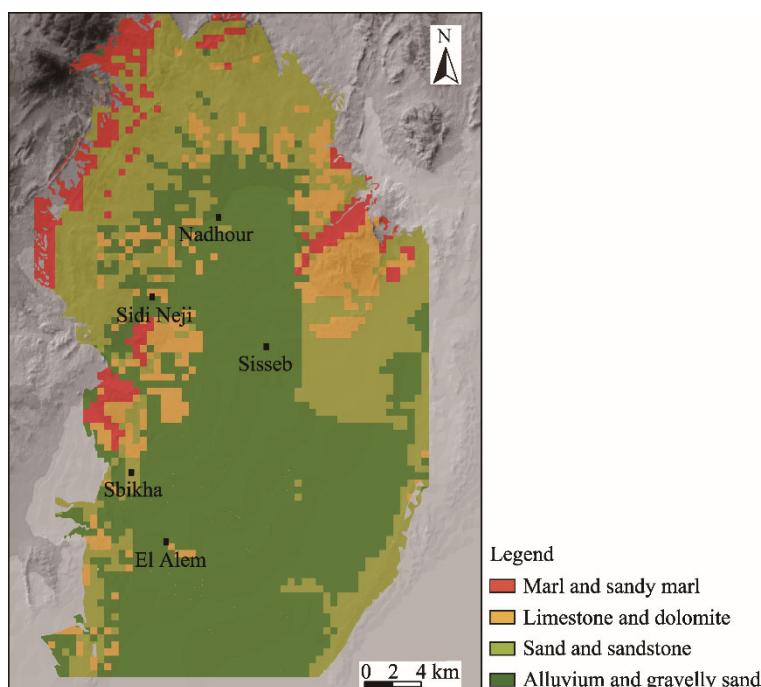
Fig. 5　Lithology of the study area

3.1.2　Soil

Infiltration is mostly affected by the soil estate near the surface (Hillel, 1982; Lowery et al., 1997). Soil texture is the main factor affecting infiltration (Hillel, 1982). Water flows faster through the larger pores of sandy soil than via the little pores of clay soil. Porous soil allow water to flow-in and to recharge underground aquifers. The soil map was generated based on the pedological map (1:500,000) of Tunisia.

The PR of the soil surface map (Table 3) was determined by calculating the correspondence values for each class. Building area received a PR value of 0.00. Mineral soil and wadi beds had a PR value of 1.00 (Table 3). PR values of the other classes were between 0.00 and 1.00.

Soil of the study area was subdivided into five classes, including building, hydromorphic and allomorphic soils, poor soils, rendzine soils and mineral soil and wadi beds (Fig. 6). Soils and mineral soil and wadi beds occupied 36% of the study area. Rendzine soil located in the upstream occupied 29% of the study area. Poor soils occupied 17% of the study area.

3.1.3　Slope

The topography inclination influences the infiltration (Al Saud, 2010) by control the intensity of water flow. It influences flow velocity, concentration time, transport of sediment and vertical and lateral digging in the wadi beds (Zaoui, 2009). For the steep slope, water runs rapidly on the surface and produces a smaller recharge rate (Yeh et al., 2009). The gentle slope increases water infiltration into the soil. Slope gradient map was done by using the slope algorithm in hydrology tools through the ArcGIS 10.1.

The slope values ranged from 0% to 44% (Table 3). The flat terrain had PR value of 1.00 and the terrain with slope 44% had a PR value of 0.00, and PR values of the other classes were between 0.00 and 1.00 (Table 3). The slope was reclassified by a negative linear equation, $f(x)= -0.022x+1$ ($x \in [0-44]$), where x is slope.

The slope values ranged from 3.4% to 44.0% (Fig. 7). The slope values were subdivided into four classes, including 0.0%–3.4%, 3.4%–9.4%, 9.4%–18.0% and 18.0%–44.0%. The class with slope values of 0.0%–3.4% represented 80% of the total study area. The slope values were high at the north and west part of the study area, while slope values were very low and close to zero at the south and center part of the study area.
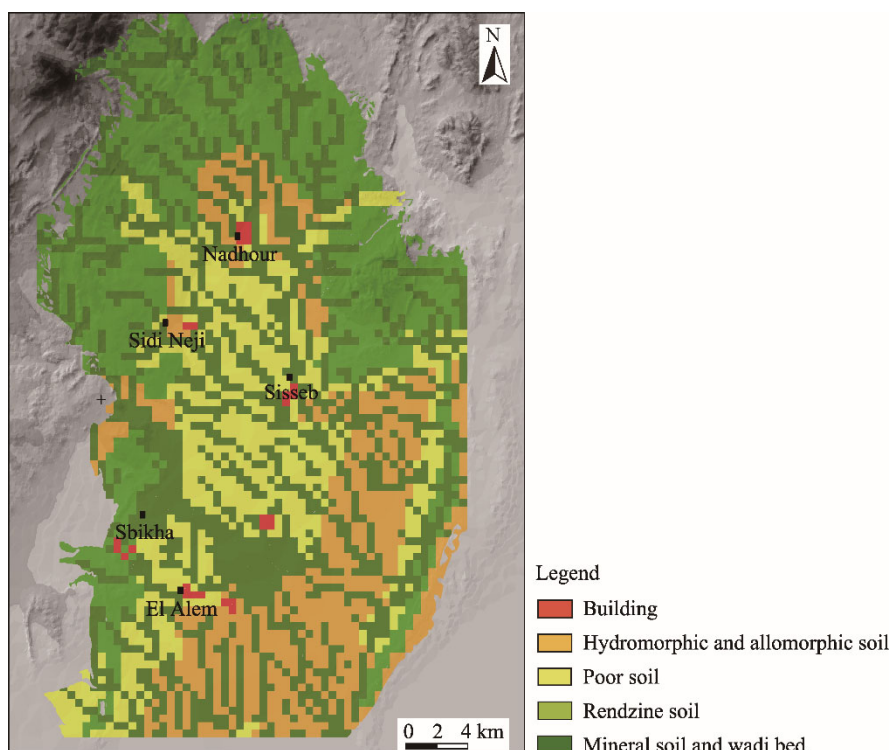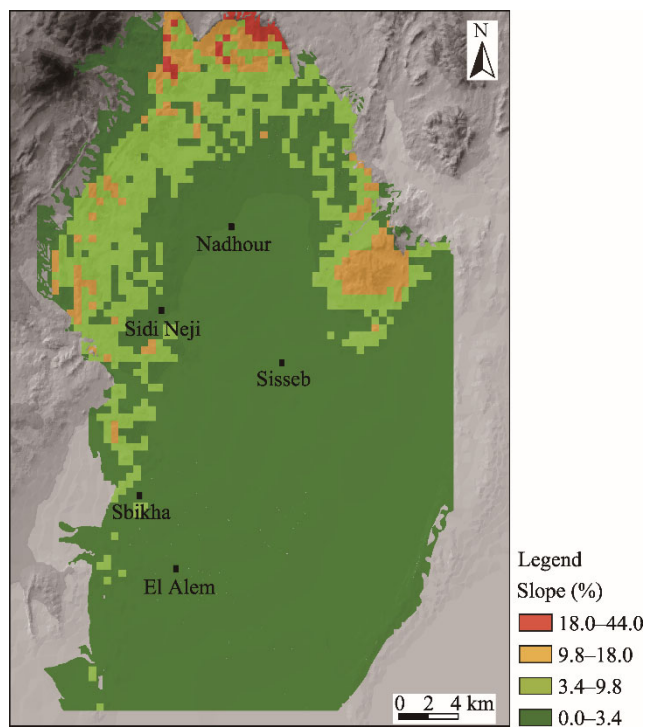
Fig. 6   Soil of the study area

Fig. 7   Slope gradient map of the study area

3.1.4   Topography

Topography (Toth, 1963), hydraulic conductivity and geology (Freeze and Witherspoon, 1967) define the hydrological landscape and hydraulic function of the basin (Winter, 2001). The

topography (relief and the variation of wavelength) of the basin controls the direction and intensity of groundwater flow (Haitjema and Mitchell-Bruker, 2005; Bresciani, 2011). In fact, where the water table intercepts the topography, the seepage condition is highlighted and a discharge area occurs in this place. These conditions influence not only the flow direction, but also the effective recharge since the aquifer outcrop areas reduce the infiltration area. The aquifers exposed in the low topographic zone make a discharge area (Bresciani, 2011). The steeper slope implies a smaller seepage area.

Topography values ranged from 2 to 500 m in the study area. The flat terrain was attributed the PR value of 0.00, the higher elevation of 500 m was attributed the PR value of 1.00, and the other classes were attributed PR values between 0.00 and 1.00. The topography was reclassified by a linear equation, $f(x)=0.002x$ ($x \in [0–500]$), where x is topography.

The topography map shows that topography values ranged from 2 to 500 m (Fig. 8). Topography was divided into five categories: a very low topography with elevation<100 m, representing 59.0% of the study area; a low topography with elevation between 100 and 200 m, representing 26.0% of the study area; an average topography with elevation between 200 and 300 m, representing 14.0% of the study area; a high topography with elevation between 300 and 400 m, representing 2.0% of the study area; and a very high topography with elevation above 400 m, representing less than 0.1% of the study area (Fig. 8).
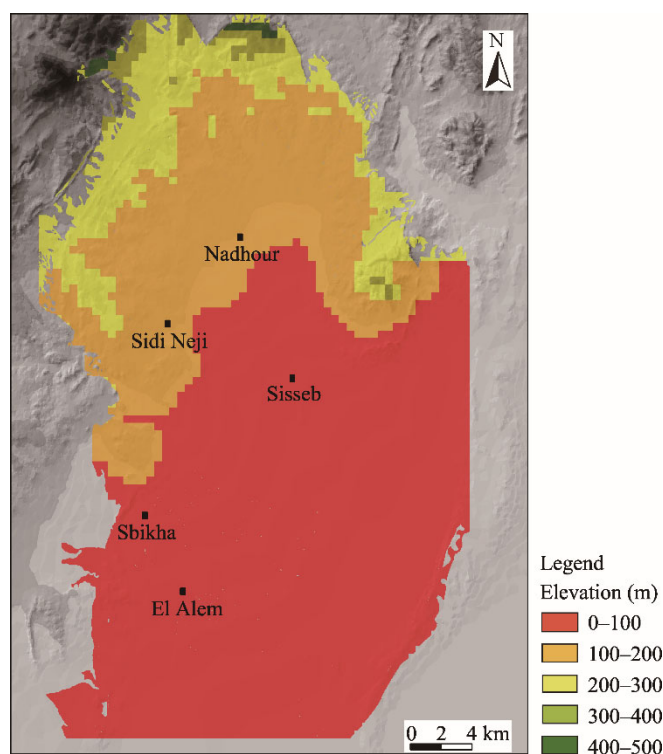

Fig. 8 Topography of the study area

3.1.5 Land cover/use

The land cover/use map was generated by using the satellite images through the ArcGIS 10.1. The recharge rate is related to land cover/use (Leduc et al., 2001). Vegetation increases the infiltration rates (Shaban et al., 2006). Effectively, biological activities; burrow creations and root decomposition help to unpack the rock and soil. This facilitates infiltration and percolation of water.

Vegetation decrease direct water evaporation (Wang et al., 2018) and slows the water runoff Water absorbed by the plant reduces water loss. Urban area decreases the infiltration rate and

increases runoff. Natural hydrological processes such as infiltration are influenced by land cover changes caused by mainly human activities; agriculture expansion, deforestation, construction works and urbanization.

The surface water body admitted a PR value of 1.00, those building had a PR value of 0.00 (Table 3). PR values of the other classes were between 0.00 and 1.00. The land cover/use map was dominated by the agricultural and bare Land. The forest, building and water areas occupied 0.04% (4.25 km^2), 0.01% (4.25 km^2) and 0.01% (5.50 km^2) of the study area, respectively (Fig. 9).
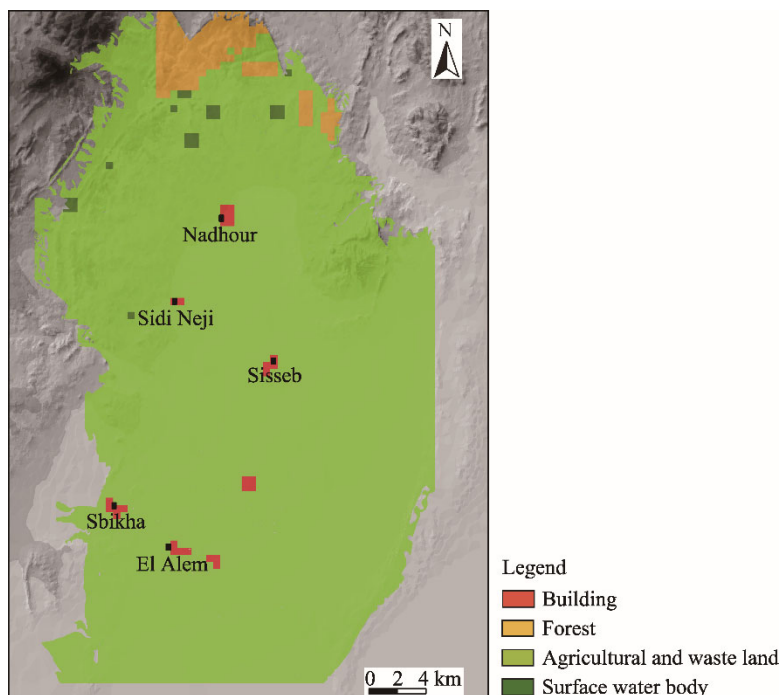
Fig. 9   Land cover/use of the study area

3.1.6   Drainage density

The drainage network was mapped from SRTM by using an algorithm for automatic extraction, flow accumulation algorithms in hydrology tools through the ArcGIS 10.1. The drainage density represents the number of segments per unit of the study area (Greenbaum, 1985). In the present study, drainage density was determined by applying the line density algorithms in the ArcGIS 10.1. Drainage density has an inverse role as permeability (Luo, 1900; Harlin and Wijeyawickrema, 1985). Indeed, a zone with an important drainage density designate less infiltration (Machiwal et al., 2011), which favors runoff and therefore acts as a poor prospect of groundwater.

Drainage density values ranged from 0.15 to 2.50 segment per km^2. The drainage densities<0.15 segment per km^2 received a PR value of 1.00 (Table 3). The drainage densities>2.5 segment per km^2 assigned a PR value of 0.00. The drainage densities between 0.15 and 0.25 segment per km^2 assigned PR values between 1.00 and 0.00 by the application of a negative linear equation, $f(x)= -0.04x+1$ ($x\in[0.0–2.5]$), where x is drainage density.

The drainage density map shows that drainage density values ranged from 0.15 to 2.50 segment per km^2 (Fig. 10). It was divided into four categories: a very low drainage density area with the value<0.62 segment per km^2; a low drainage density area with the value between 0.62 and 1.25 segment per km^2; a zone with an average drainage density with the value between 1.25 and 1.87 (segment per km^2); and a high drainage density are with the value above 1.87 segment per km^2. The drainage density map shows that the basin was dominated by the average drainage density areas which occupied 48% of the study area. The low and high drainage density areas occupied 24% and 21% of the study area, respectively. This indicates a large extension of the recharge area. Areas

with low drainage density occupy the upstream at the outcrop of sandstone and sand.
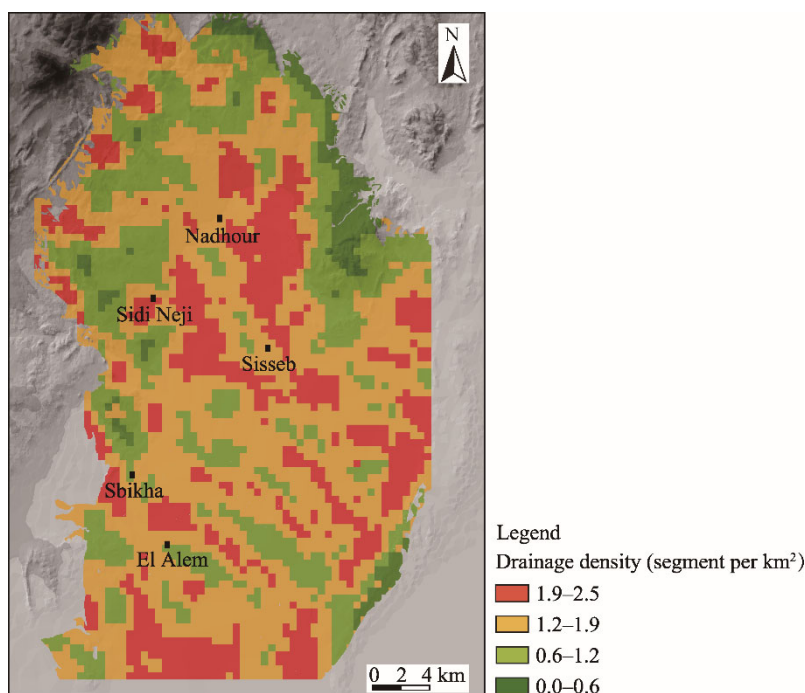

Fig. 10   Drainage density of the study area

3.1.7   Lineament

The lineament density map was generated by the automatic extraction process from satellite images (Souei et al., 2017). The lineament density is the number of lineament per unit of the study area (Fig. 11). It is a secondary porosity and increases with the density representing the area with good groundwater potential. It is determined by applying the line density algorithm in ArcGIS 10.1.

The lineament density map shows that values of lineament density varied between 0 and 45 (lineament per km^2). The lineament density of 45 lineament per km^2 took a PR value of 1.00 and of less than 45 lineament per km^2 took a PR value from 0.00 to 1.00 (Table 3). The lineament class was determined by a positive linear equation, $f(x)=0.022x$ ($x \in [0–45]$), where x is lineament density.

The lineaments density was divided into three classes: a very low lineament density class with a value of 0–10 lineament per km^2, representing 64% of the study area; a low lineament density class with a value between 10 and 30 lineament per km^2, representing 26% of the study area; and a high lineament density class with a value between 30 and 45 lineament per km^2, occupying the basin borders and superimposed on majorities with sandstones and sand outcrops. The very low lineament density class took over the entire lower topographic zone of the study area.

3.1.8   Runoff

Runoff occurs when precipitation intensity exceeds infiltration and soil surface retention capacity (Larue, 2000; Sauvadet et al., 2012). The threshold for the onset of runoff varies according to the height and intensity of rainfall, soil moisture, soil surface conditions (fissures, pebbles, clods, etc.), vegetation cover and physical properties of the soil (porosity and organic matter content) (Morsli et al., 2004). Lithomorphic soils, marls, clays and impermeable soils of urban areas (e.g., roads, car parking, built-up areas, etc.) increase runoff at the expense of infiltration (Morsli et al., 2004; Sauvadet et al., 2012). The PR of Runoff was defined by the determination of the correspondence rate for each class. Building area with high runoff admitted a PR value of 0.00 (Table 3). Wadi beds with high infiltration had a PR value of 1.00 (Table 3). PR values of the other classes were between 0.00 and 1.00.
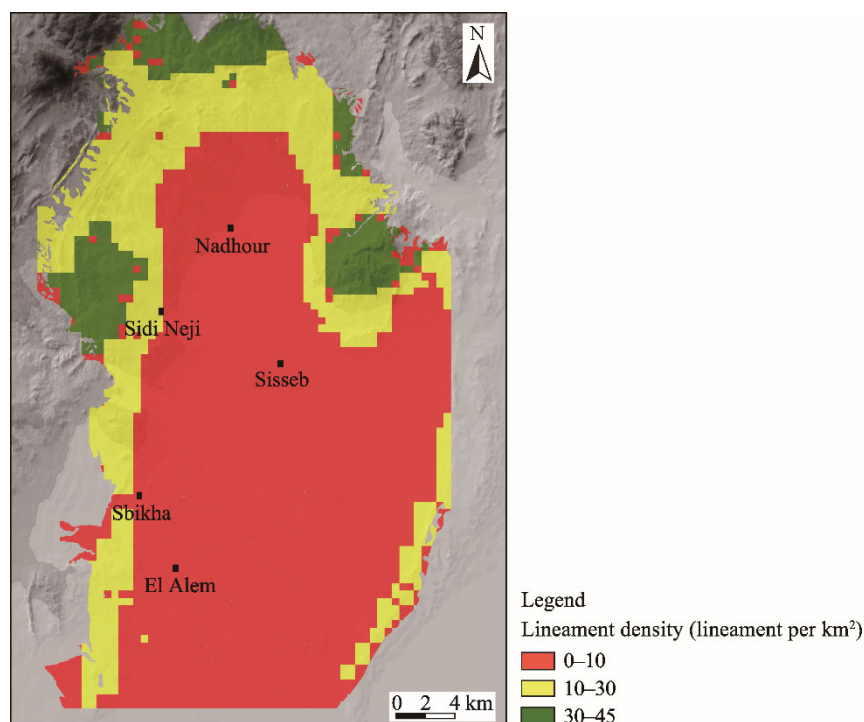
Fig. 11　Lineament density of the study area

The study area was dominated by the wadi deposit (34.00% of the total study area). The central part of the basin was dominated by alluvial deposits (30.00% of the total study area) (Fig. 12). The hilly areas were represented by a sand and sandstone deposit (22% of the total study area). The limestone and dolomites with fractures, marl, clay and building areas represented 7.00%, 6.00% and 0.01% of the study area, respectively.

3.2　Determined consistency ratio (CR) and the sensitivity analysis

CR was calculated as follows:

$$CR = \frac{CI}{RI}, \tag{8}$$

where RI is the Random index, whose value associated with the number of factors (n) (Saaty, 1980), RI=1.41 (Table 4). According to Equation 5, CI=0.002. Then, CR=0.001. The calculated CR value was less than 0.10, indicating that there is a realistic degree of consistency in the pair-wise comparison (Saaty, 1980).

Table 4　Arbitrary index based on the number of criteria (Saaty, 1980)

n	5	6	7	8	9	10	11	12
RI	1.12	1.24	1.32	1.41	1.45	1.49	1.51	1.54

Note: n, number of factors; RI, random index.

The sensitivity analysis showed that in the assessment of potential groundwater recharge index, lithology and soil presented the most important factor as their effective weight (22% and 20%, respectively) (Table 5) exceeded the theoretical weight (17%). The sensitivity analysis indicated that lithology, soil, slope and topography were underestimated. However, land cover/use, drainage density, lineaments density and runoff were overestimated (Table 5).

3.3　Groundwater recharge potential areas

The obtained recharge indices were classified into five potential classes as poor, low, moderate, good and very good (Fig. 13). Figure 13 indicates that very good potential areas only covered 27%
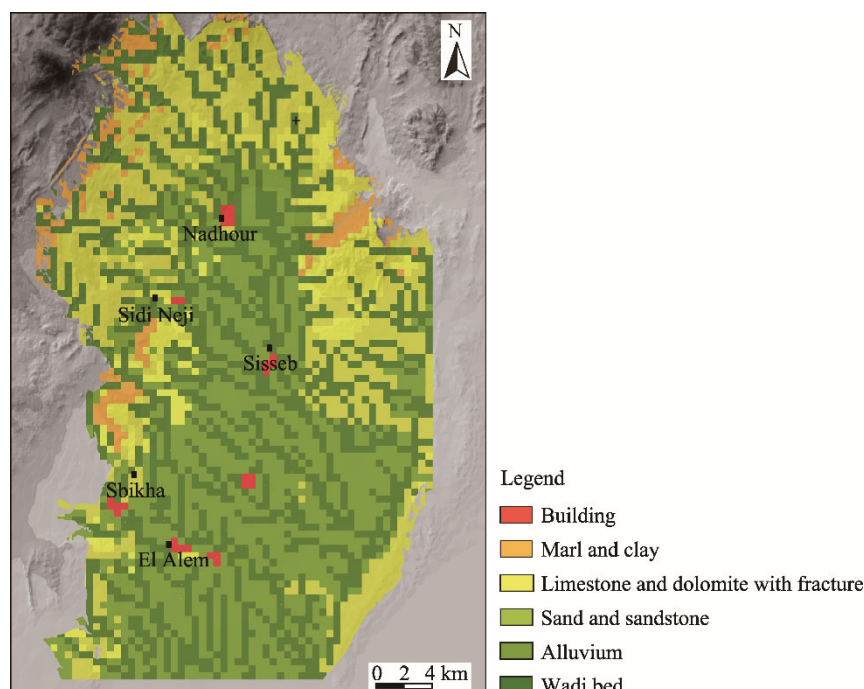
Fig. 12 Runoff of the study area

Table 5 Single parameter sensitivity analysis

Factor	Theoretical weight		Effective weight			
	Value	Proportion (%)	Mean (%)	Min (%)	Max (%)	SD (%)
Li	4.5	17	22	7	45	17
S	4.5	17	20	3	39	16
Sl	3.5	13	14	1	41	17
T	3.5	13	14	7	33	11
LU/C	3.5	13	12	3	51	22
Dd	3.0	11	8	1	56	24
Ld	2.5	9	8	12	53	21
Ru	1.5	6	2	2	31	11

Note: Min, minimum; Max, maximum; SD, standard deviation.

of the study area. It was in the upstream and the southwest parts of the basin. Also, the areas with very good infiltration potential were mainly represented by wadi beds. The good infiltration class was located in the north and center of the basin, occupied about 44% of the study area and scattered all over the basin. Moderate infiltration class were mainly situated in the southeast and south parts of the basin and occupied 17% of the study area. Potentially poor and low classes occupied about 12% of the study area.

3.4 Experimental validation and infiltration rate

After the establishment of the groundwater recharge potential areas, a validation of the used method followed by an estimate of natural infiltration rate was necessary. To achieve these objectives, the control data from three artificial recharge operation were used. The recharge campaigns were carried out since the Saidaine hill dam in the streambed of the Saadine wadi (Fig. 13). These operations consisted of dropping water continuously over a period of time. The detail data of the three artificial recharge operations are shown in Table 6. The recharge operation was controlled by data measurement in four control stations (S1, S2, S3 and S4) located along the 11 km path from the streambed.
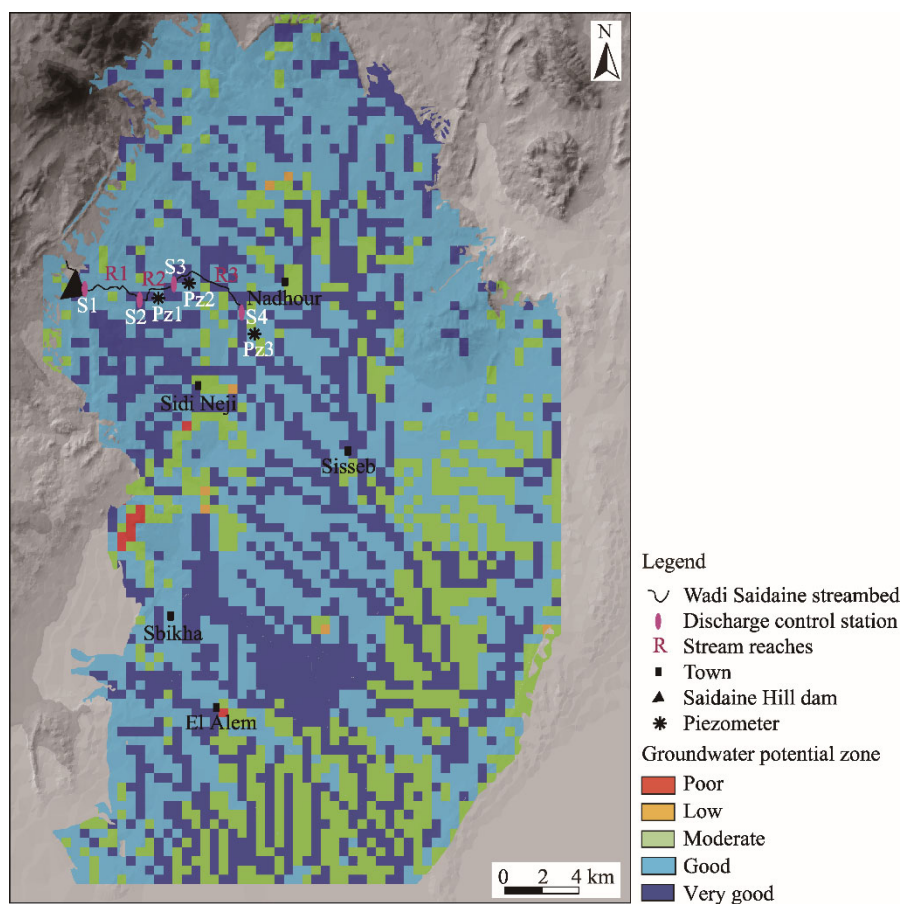
Fig. 13 Groundwater recharge potential areas. WRI, water recharge index.

The locations of these stations were shown in Figure 13. Along the submersed wadi bed area, three reaches were defined (R1, R2 and R3) from the upstream to downstream. The average area of submersed zone was 0.115 km² (Ibn Ali et al., 2017). The measuring of difference between upstream and downstream water flows in the four control stations can determine the infiltration and evapotranspiration rates in the three reaches. It was determined as average values of the three campaigns for the three reaches (Table 6).

Indeed, for more precision, the potential evaporation (PE) measured at the Kairouan meteorological station during the recharge operations (2004, 2005 and 2006) were used. In general, the average PE was 7% compared to the artificial recharge volume (Table 7). Statistical analysis of the three artificial recharge shows that the mean infiltration capacities of reaches R1, R2 and R3 were 32%, 57% and 80%, respectively. The results show that the reach R1 is the zone with good recharge index (Fig. 13), whereas the reaches R2 and R3 are the zones with very good recharge index.

The average infiltration capacity of the reaches R2 and R3 is 69% and the average infiltration capacity of reaches R1 and R2 is 45%. Indeed, the 69% infiltration capacity is attributed to a very good recharge index class and 45% infiltration capacity is attributed to a good recharge index class. The infiltration capacity for the other classes was determined arbitrarily (Table 8). To estimate the infiltration rate, the infiltration capacity of each recharge index class was determined (Table 8).

The natural infiltration rate was calculated by multiplying the precipitation by the infiltration capacity (Table 8). The average precipitation used in the estimate of infiltration rate was 364 mm. It was corresponding to the average annual precipitation for the period 1997–2013 (Fig. 14). The result shows that the infiltration capacity (an average annual of 167×10^6 m³) in the study area was 43% of the total precipitation (Table 8).

Table 6 Details of the three artificial recharge operations

Period	4 Feb–17 Aug 2004				11 Feb–4 Aug 2005				25 Feb–15 Aug 2006			
Station	S1	S2	S3	S4	S1	S2	S3	S4	S1	S2	S3	S4
NM	51	45	28	-	39	38	38	25	32	31	31	7
VM ($\times10^6$ m^3)	1.615	0.740	0.105	-	2.542	2.023	1.296	0.347	1.675	1.292	0.641	0.081
Reach	-	R1	R2	R3	-	R1	R2	R3	-	R1	R2	R3
VL ($\times10^6$ m^3)	-	0.875	0.635	-	-	0.519	0.727	0.949	-	0.383	0.651	0.560
PVL (%)	-	54	86	-	-	20	36	73	-	23	50	87

Note: NM, number of measurements; VM, volume measured; VL, volume lost; PVL, percentage of volume lost by the reach; -, data not available.

Table 7 Determination of the potential evaporation (PE) in Kairouan meteorological station

Period	Submersed bed area ($\times10^3$ m^2)	Artificial recharge ($\times10^6$ m^3)	PE		
			(mm)	($\times10^6$ m^3)	(%)
Feb–Aug 2004		1.6	11.11	0.127	8
Feb–Aug 2005	115	2.5	1.19	0.136	5
Feb–Aug 2006		1.7	1.26	0.145	9

Table 8 Determination of the infiltration rate

Groundwater recharge potential index	Infiltration capacity	Average precipitation for the period 1997–2013 (mm/a)	Percentage of the area (%)	Infiltration+PE ($\times10^6$ m^3/a)	PE ($\times10^6$ m^3/a)	Infiltration ($\times10^6$ m^3/a)
Poor	0.04		1	3.64	0.25	3.39
Low	0.17		11	7.86	0.55	7.31
Moderate	0.31	364	17	20.30	1.42	18.88
Good	0.45		44	76.30	5.34	70.96
Very good	0.69		27	71.79	5.03	66.76
Total			100	179.89	12.59	167.30

4 Discussion

The present work confirmed the importance of the compilation of statistics methods, GIS and remote sensing in the determination of multidisciplinary method favorable in the delimitation of groundwater recharge potential areas. The use of fuzzy logic presented a more sophisticated and simple process to increase the degree of decision. Using Fuzzy logic process in the determination of the order of importance of factors and class becomes easier than using other process based on linguistic and vague patterns. The eight factors used were carefully selected to take into account the specificity of the region and the condition occurring in the aquifer water supply. Other methods used fewer factors. The decrease in the number of factors affects the degree of precision.

The determination of infiltration rate based on experimental data showed that the benefits of the intervention in the management of these zones were determined on the map. The infiltration map, Figure 13, presented a basic document of all future management in the basin. This study allowed the decision makers to choose the sites of intervention to compensate the pizometric drop existing in the basin, also to occur in the protection of the aquifer system against pollution. Despite its efficiency, this method took a time in the processing of the data, whether for the assembly of the raw data or during the processing of the rectification of the data.

The use of more accurate and detailed experimental data, some field studies makes it possible to improve results better. The programming of the method by computer system allows to accelerate the processes of establishment of the final result and to integrate the database and the results in the hydrodynamic mathematical modeling of the aquifer system.

5 Conclusions

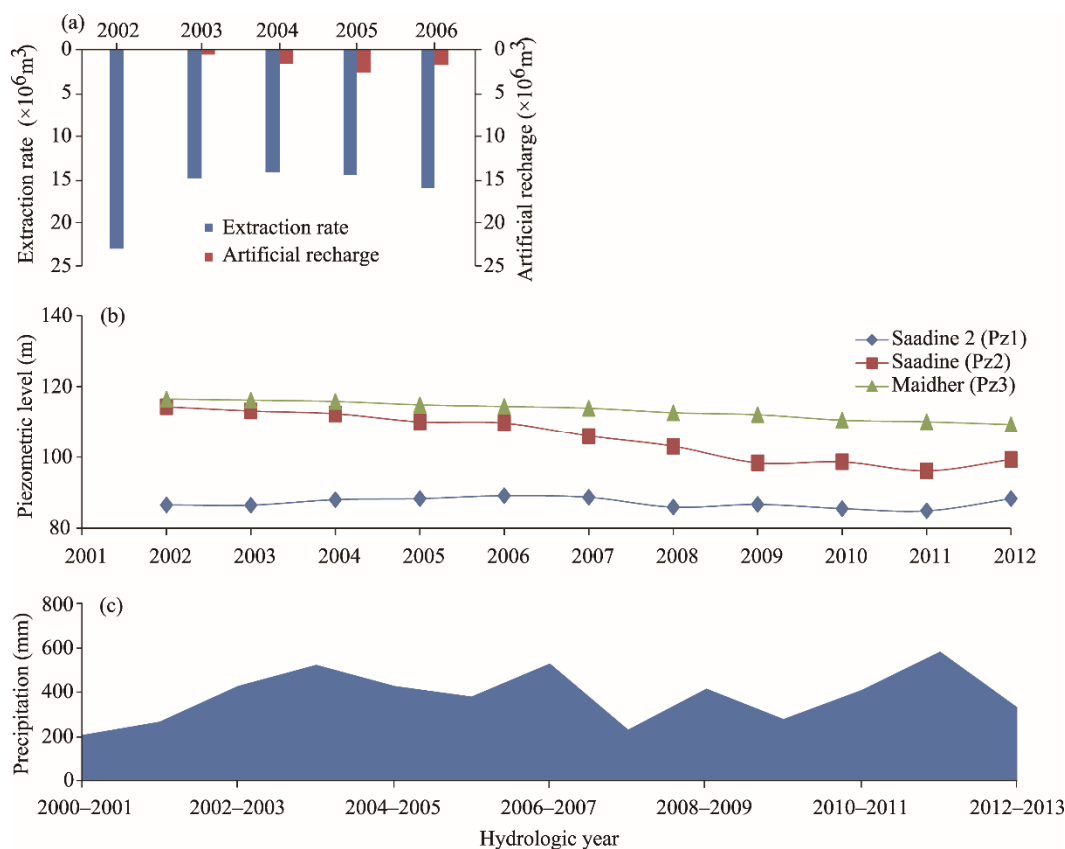Groundwater recharge potential area map is proposed for the Nadhour-Sisseb-El Alem Basin. The

Fig. 14 Aquifer recharge and groundwater extraction (GWRD, 2013a) (a); temporal variation of the piezometric level (GWRD, 2012) (b); and average annual precipitation (c) (GWRD, 2013b).

statistical method allows investigating the influence of geomorphological, climatic, geological and hydrological factors on the recharge of the aquifer. Indeed, this study demonstrates that the groundwater recharge index is more correlated with lithology and drainage. The quantity of supplies water from groundwater remains essentially linked to the climatic condition of the study area. The superposition of several layers of information, using GIS has allowed to develop a digital map supports for integrated water resources management. Indeed, this methodology allowed proposed recharge zones to remedy the alarming situation of the overexploited aquifers. The calibration of theoretic method with the artificial recharge operation confirms the utility of used method in the determination of the potential recharge areas. The natural infiltration capacity (an average of 167×10^6 m³/a) was 43% of the total precipitation.

The study clearly shows the interest in the use of spatial techniques, offered by GIS and remote sensing for hydrological study. Utilization of this method detailed in this work can be helpful to map the recharge area in others regions essentially the regions characterized by the difficult accessibility. This method is also applicable to delineation other natural disaster as the flood risk.

Acknowledgements

References

Al Saud M. 2010. Mapping potential areas for groundwater storage in Wadi Aurnah Basin, western Arabian Peninsula, using remote sensing and geographic information system techniques. Hydrogeology Journal, 18: 1481–1495.

Aouragh M H, Essahlaoui A, El Ouali A, et al. 2016. Groundwater potential of Middle Atlas plateaus, Morocco, using fuzzy logic approach, GIS and remote sensing. Geomatics, Natural Hazards and Risk, 8(2): 194–206.

Ayadi M. 2014. Artificial recharge of underground aquifers in Tunisia. In: Ministry of Agriculture and Hydraulic Resources. General Water Resources Direction Report Note TN190. Tunis, Tunisia. (in French).

Bresciani E. 2011. Modeling of climatic, topographic, geological and anthropogenic controls on underground flows in the basement area. PhD Dissertation. La Chapelle-Thouarault: University Rennes 1. (in French).

Buckley J J. 1984. The multiple judge, multiple criteria ranking problem: a fuzzy set approach. Fuzzy Sets and Systems, 13(1): 25–37.

Chenini I, Ben Mammou A, El May M. 2010. Groundwater recharge zone mapping using GIS-based multi-criteria analysis: a case study in Central Tunisia (Maknassy Basin). Water Resources Management, 24: 921–939.

Elewa H H, Qaddah A A. 2011. Groundwater potentiality mapping in the Sinai Peninsula, Egypt, using remote sensing and GIS-watershed-based modeling. Hydrogeology Journal 19: 613–628.

Freeze R A, Witherspoon P A. 1967. Theoretical analysis of regional groundwater flow: 2. Effect of water-table configuration and subsurface permeability variation. Water Resources Research, 3(2): 623–634.

Greenbaum D. 1985. Review of remote sensing applications to groundwater exploration in basement and regolith. British Geological Survey. Nottingham, UK.

GWRD. 2012. Piezometric level of underground aquifers in Tunisia. In: General Water Resources Direction Report Note TN180. Tunis, Tunisia. (in French)

GWRD. 2013a. Precipitation in Tunisia. In: General Water Resources Direction Report Note TN179. Tunis, Tunisia. (in French)

GWRD (General Water Resources Direction). 2013b. Aquifer recharge and groundwater extraction. In: General Water Resources Direction Report Note TN380. Tunis, Tunisia. (in French)

Haitjema H M, Mitchell-Bruker S. 2005. Are water tables a subdued replica of the topography? Ground Water, 43(6): 781–786.

Harlin J M, Wijeyawickrema C. 1985. Irrigation and groundwater depletion in Caddo County, Oklahoma. Journal of the American Water Resources Association, 21(1): 15–22.

Hillel D. 1982. Introduction to Soil Physcics. San Diego: Academic press. 22.

Ibn Ali Z, Triki I, Lajili-Ghezal L, et al. 2017. A method to estimate aquifer artificial recharge from a hill dam in Tunisia. Journal of Arid Land, 9(2): 244–255.

Jaiswal R K, Mukherjee S, Krishnamurthy J, et al. 2003. Role of remote sensing and GIS techniques for generation of groundwater prospect zones towards rural development an approach. International Journal of Remote Sensing, 24(5): 993–1008.

Jasrotia A S, Bhagat B D, Kumar A, et al. 2013. Remote sensing and GIS approach for delineation of groundwater potential and groundwater quality zones of western Doon Valley, Uttarakhand, India. Journal of the Indian Society of Remote Sensing, 41: 365–377.

Jha M K, Chowdhury A, Chowdary V M, et al. 2007. Groundwater management and development by integrated remote sensing and geographic information systems: prospects and constraints. Water Resources Management, 21: 427–467.

Kallali H, Anan M, Jellali S, et al. 2007. GIS-based multi-criteria analysis for potential wastewater aquifer recharge sites. Desalination, 215(1–3): 111–119.

Kirpich Z P. 1940. Time of concentration of small agricultural watersheds. International Journal of Civil Engineering, 10(6): 362.

Krishnamurthy J, Mani A, Jayaraman V, et al. 2000. Groundwater resources development in hard rock terrain: An approach using remote sensing and GIS techniques. International Journal of Applied Earth Observation and Geoinformation, 2(3–4): 204–215.

Larue J P. 2000. Contribution of concentrated runoff to the erosion of cultivated sandy soils in the west of the Paris Basin: the example of the Dué and Narais basins. Ingenieries-EAT, 21: 51–62. (in French)

Leberling H. 1981. On finding compromise solutions in multicriteria problems using the fuzzy min-operator. Fuzzy Sets and Systems, 6(2): 105–118.

Leduc C, Favreau G, Schroeter P. 2001. Long-term rise in a Sahelian water-table: the Continental Terminal in South-West Niger. Journal of Hydrology, 243(1–2): 43–54.

Lowery B, Hickey W J, Arshad M A, et al. 1997. Soil water parameters and soil quality. In: Doran J W, A J Jones. Methods for Assessing Soil Quality. Madison: Soil Science Society of America, Inc., 143–155.

Luo W. 1900. Quantifying groundwater-sapping landforms with a hypsometric technique. Journal of Geophysical Research, 105(E1): 1685–1694.

Machiwal D, Jha M K, Mal B C. 2011. Assessment of groundwater potential in a semi-arid region of India using remote sensing, GIS and MCDM techniques. Water Resources Management, 25: 1359–1386.

Madrucci V, Fabio T, de Araújo C C. 2008. Groundwater favorability map using GIS multicriteria data analysis on crystalline terrain, São Paulo State, Brazil. Journal of Hydrology, 357(3–4): 153–173.

Morsli B M, Mazour N, Mededjel A H, et al. 2004. Influence of land use on the risks of runoff and erosion on the semi-arid area of northwestern Algeria. Drought, 15(1): 96–104. (in French)

Napolitano P and Fabbri A. 1996. Single-parameter sensitivity analysis for aquifer vulnerability assessment using DRASTIC and SINTACS. In: HydroGIS 96: Application of Geographical Information Systems in Hydrology and Water Resources Management, Proceedings of Vienna Conference. Vienna: IAHS Pub, 235: 559–566.

Preeja K R, Joseph S, Thomas J, et al. 2011. Identification of groundwater potential zones of a tropical river basin (Kerala, India) using remote sensing and GIS techniques. Journal of the Indian Society of Remote Sensing, 39: 83–94

Rashid M, Lone M, Ahmed S. 2012. Integrating geospatial and ground geophysical information as guidelines for groundwater potential zones in hard rock terrains of south India. Environmental Monitoring and Assessment, 184: 4829–4839.

Rahman A, Kumar S, Fazal S, et al. 2012. Assessment of land use/land cover change in the north-west district of Delhi using remote sensing and GIS techniques. Journal of the Indian Society of Remote Sensing, 40: 689–697.

Rezaei F, Hamid R, Safavi D, et al. 2013. Groundwater vulnerability assessment using fuzzy logic: A case study in the Zayandehrood Aquifers, Iran. Environmental Management, 51: 267–277.

Riad P H, Billib M H, Hassan A A, et al. 2011a. Water scarcity management in a semi-arid area in Egypt: overlay weighted model and Fuzzy logic to determine the best locations for artificial recharge of groundwater. Nile Basin, Water Science and Engineering Journal, 4(1): 24–35.

Riad P H, Billib M, Hassan A A, et al. 2011b. Application of the overlay weighted model and Boolean logic to determine the best locations for artificial recharge of groundwater. Journal of Urban and Environmental Engineering, 5(2): 57–66.

Rognon P. 2000. How to develop artificial groundwater recharge in dry regions. Drought, 11: 289–296. (in French)

Saaty T L. 1980. The Analytic Hierarchy Process: Planning, Priority Setting, Resource Allocation. New York (NY): McGraw-Hill International Book Company.

Sauvadet M, Raclot DA, Ben Slimane A, et al. 2012. Determinism of runoff and water erosion from the plot to the slope in a marly Mediterranean environment. Moroccan Journal of Agronomic and Veterinary Sciences, 1: 41–46. (in French)

Shaban A, Khawlie M, Abdallah C. 2006. Use of remote sensing and GIS to determine recharge potential zones: the case of Occidental Lebanon. Hydrogeology Journal, 14: 433–443.

Souei A. 2012. Geophysical and hydrogeological characterization of the aquifer systems of the Sisseb-El Alem basin, Central-eastern Tunisia. MSc Thesis. Tunis: University of Tunis El Manar. (in French)

Souei A, Zouaghi T. 2017. Use of GIS for the integrated management of water resources in the region of Central-Eastern Tunisia: Kairouan Nord. Arid Regions Review, 41(1): 265–268. (in French)

Souei A, Mhimdi S, Zouaghi T. 2017. Extraction by remote sensing of fracture networks in the region of Sisseb-El Alem; North Kairouan; hydrogeological implication. In: Abstracts of the 1st Atlas Georesources International Congress. Hammamet: LGR, 20–22. (in French)

Souei A, Atawa M, Zouaghi T. 2018. Hydrogeological framework and geometry modeling via joint gravity and borehole parameters, the Nadhour-Sisseb-El Alem Basin (central-eastern Tunisia). Journal of African Earth Sciences, 139: 133–164.

Souei A, Zouaghi T. 2018. 2D seismic reflection contribution to structural and geometric study of Cenozoic aquifer systems in the Sisseb El-Alem basin, central-eastern Tunisia. Arabian Journal of Geosciences 11: 689.

Souei A. 2019. Contribution of geophysics, remote sensing, GIS, and hydrochemistry to the hydrological and hydrogeological study of aquifer systems in the Nadhour-Sisseb-El Alem basin; Central Eastern Tunisia. PhD Dissertation. Tunis: Tunis-El Manar University.

Souei A, Atawa M, Zouaghi T. 2021. 3D seismic velocities modeling and its application in the appreciation of the complex deep framework; the Sisseb-El Alem basin, central-eastern Tunisia. Arabian Journal of Geosciences. 14, 2001 (2021). https://doi.org/10.1007/s12517-021-08300-y.

Toth J. 1963. A theoretical analysis of groundwater flow in small drainage basins. Journal of Geophysical Research, 68(16): 4795–4812.

Tweed S O, Leblanc M, Webb J A, et al. 2007. Remote sensing and GIS for mapping groundwater recharge and discharge areas

in salinity prone catchments, southeastern Australia. Hydrogeology Journal, 15(1): 75–96.

Wang Y, Liu Y, Jin J. 2018. Contrast effects of vegetation cover change on evapotranspiration during a revegetation period in the Poyang Lake Basin, China. Forests, 9(4): 217.

Winter T C. 2001. The concept of hydrologic landscapes. Journal of the American Water Resources Association, 37(2): 335–349.

Yeh H F, Lee C H, Hsu K C, et al. 2009. GIS for the assessment of the groundwater recharge potential zone. Environmental Geology, 58: 185–195.

Yeh H F, Cheng YS, Lin H I, et al. 2016. Mapping groundwater recharge potential zone using a GIS approach in Hualian River, Taiwan. Sustainable Environment Research, 26(1): 33–43.

Zadeh L A. 1965. Fuzzy sets. Information and Control, 8(3): 338–353.

Zadeh L A. 1987. A computational theory of dispositions. International Journal of Intelligent Systems, 2: 39–63.

Zaoui S. 2009. Contribution of GIS in the study of the sub-watershed of Sidi Ayad (Haute Moulouya, Morocco). MSc Thesis. Meknes: Moulay Ismail University. (in French)